



# Tsc1 regulates tight junction independent of mTORC1

Mingqiang Lai<sup>a,1</sup>, Wenchong Zou<sup>a,1</sup>, Zelong Han<sup>b,1</sup> , Ling Zhou<sup>a</sup> , Zeyou Qiu<sup>a</sup> , Juan Chen<sup>a</sup>, Sheng Zhang<sup>a</sup>, Pinglei Lai<sup>c</sup>, Kai Li<sup>c</sup>, Yue Zhang<sup>a</sup> , Li Liang<sup>d</sup>, Yu Jiang<sup>e</sup>, Zhipeng Zou<sup>a,2</sup> , and Xiaochun Bai<sup>a,c,f,2</sup> 

<sup>a</sup>State Key Laboratory of Organ Failure Research, Department of Cell Biology, School of Basic Medical Sciences, Southern Medical University, Guangzhou 510515, China; <sup>b</sup>Guangdong Provincial Key Laboratory of Gastroenterology, Department of Gastroenterology, Nanfang Hospital, Southern Medical University, Guangzhou 510515, China; <sup>c</sup>Guangdong Provincial Key Laboratory of Bone and Joint Degeneration Diseases, Academy of Orthopedics, The Third Affiliated Hospital of Southern Medical University, Guangzhou 510630, China; <sup>d</sup>Department of Pathology, School of Basic Medical Sciences, Southern Medical University, Guangzhou 510515, China; <sup>e</sup>Department of Pharmacology and Chemical Biology, University of Pittsburgh School of Medicine, Pittsburgh, PA 15261; and <sup>f</sup>Department of Basic Research and International Collaboration, Bioland Laboratory (Guangzhou Regenerative Medicine and Health Guangdong Laboratory), Guangzhou 510005, China

Edited by Leanne Jones, University of California Los Angeles, San Francisco, CA, and accepted by Editorial Board Member Brigid L. Hogan June 16, 2021 (received for review October 6, 2020)

**Tuberous sclerosis complex 1 (Tsc1) is a tumor suppressor that functions together with Tsc2 to negatively regulate the mechanistic target of rapamycin complex 1 (mTORC1) activity. Here, we show that Tsc1 has a critical role in the tight junction (TJ) formation of epithelium, independent of its role in Tsc2 and mTORC1 regulation. When an epithelial cell establishes contact with neighboring cells, Tsc1, but not Tsc2, migrates from the cytoplasm to junctional membranes, in which it binds myosin 6 to anchor the perijunctional actin cytoskeleton to  $\beta$ -catenin and ZO-1. In its absence, perijunctional actin cytoskeleton fails to form. In mice, intestine-specific or inducible, whole-body Tsc1 ablation disrupts adherens junction/TJ structures in intestine or skin epithelia, respectively, causing Crohn's disease-like symptoms in the intestine or psoriasis-like phenotypes on the skin. In patients with Crohn's disease or psoriasis, junctional Tsc1 levels in epithelial tissues are markedly reduced, concomitant with the TJ structure impairment, suggesting that Tsc1 deficiency may underlie TJ-related diseases. These findings establish an essential role of Tsc1 in the formation of cell junctions and underpin its association with TJ-related human diseases.**

Tsc1 | Myo6 | tight junction-related disease | cell adhesion | mTORC1

**E**pithelium is a thin tissue covering the body surface, lining alimentary spaces, and other structures inside the body. It is composed of a layer of attached epithelial cells, such that it blocks the paracellular diffusion of solutes and water, as well as preventing infectious microorganisms entering the body (1). This paracellular blockage is achieved by a tripartite apical junctional complex, which constitutes tight junctions (TJs), adherens junctions (AJs), and desmosomes arranged in sequential order, from the apical end to the basal end of the junction. In this arrangement, TJs establish barrier functions. Consequently, TJ dysfunction is associated with a myriad of human diseases, including Crohn's disease, ulcerative colitis, celiac disease (leak-flux diarrhea), cystic fibrosis, atopic dermatitis (AD), and psoriasis (1–3).

TJs are composed of networks of strands formed by transmembrane proteins. The extracellular domains of these membrane proteins are tethered together, and their cytoplasmic domains are anchored to the actin cytoskeleton via cytoplasmic scaffolding proteins. More than 40 different proteins have been found in TJs, including transmembrane proteins, claudins, junctional adhesion molecules, coxsackie adenovirus receptors, and TJ-associated marvel proteins, such as occludin, tricellulin, marvelD3 proteins, and cytoplasmic scaffolding proteins of the ZO family (4–7). While AJ and TJ structural components and organization are well studied, the mechanisms controlling their assembly and stability of established adhesive contacts remain unclear. Several studies have shown that AJ formation precedes TJ and is essential for TJ formation (8, 9). The attachment of the cadherin  $\alpha$ -catenin- $\beta$ -catenin adhesion complex to perijunctional cortex actin filaments establishes AJs (10, 11). The subsequent recruitment of ZO-1 to the  $\alpha$ -catenin- $\beta$ -catenin complex is believed to initiate TJ formation from the existing AJs (12).

Tsc1 (hamartin) is a tumor suppressor protein encoded by *TSC1*, a causative gene for tuberous sclerosis complex (TSC) syndrome (13–16). Tsc1 functions with Tsc2, a GTPase-activating protein (GAP), to restrict Rheb activation, a Ras-like small GTPase and activator of mechanistic targets of rapamycin complex 1 (mTORC1). Tsc1 binds Tsc2 directly to stabilize the latter, preventing it from proteasomal degradation (17, 18). The GAP activity of Tsc2 leads to Rheb inactivation and subsequent mTORC1 inhibition (19, 20). mTORC1 is a central signaling hub controlling cell growth, metabolism, survival, and autophagy in response to nutrient availability and growth factors (21–25). Its abnormal activation in Tsc1- and Tsc2-deficient cells is believed to be the main pathogenic cause behind TSC syndrome (20, 26, 27).

While studying the function of Tsc1 in intestinal epithelial cells, we serendipitously observed that intestinal, epithelial-specific Tsc1 ablation caused symptoms and histopathological alterations in mice, commonly associated with TJ defects (28, 29). This observation led us to investigate a previously unknown role of Tsc1 in TJs. Here, we show that Tsc1 is a key regulator of cell–cell adhesion that controls TJ formation independent of its role in mTORC1 regulation. Reduced Tsc1 levels at the junctional membrane are associated with TJ-related diseases in humans.

## Significance

**The epithelium barrier is vital for sealing body surface and alimentary spaces, preventing paracellular material diffusion and pathogen invasion. We describe here that tuberous sclerosis complex 1 (Tsc1) controls tight junction (TJ) formation to create and maintain the epithelial barrier, independent of its conventional role in mTOR regulation. We found that Tsc1 loss is associated with TJ destruction in patients with TJ-related human diseases, such as inflammatory bowel disease and psoriasis, a common skin disorder. Tsc1 knockout in epithelial cells drives TJ dysfunction, causing Crohn's disease-like and psoriasis-like signs and symptoms in mice. This function of Tsc1 has significant implications to understand how epithelial cells form TJ to protect us from these diseases.**

Author contributions: J.C., Z.Z., and X.B. designed research; M.L., W.Z., Z.H., L.Z., S.Z., P.L., and L.L. performed research; M.L., W.Z., Z.Q., J.C., S.Z., K.L., Y.Z., Y.J., Z.Z., and X.B. analyzed data; and Y.J., Z.Z., and X.B. wrote the paper.

The authors declare no competing interest.

This article is a PNAS Direct Submission. L.J. is a guest editor invited by the Editorial Board. Published under the [PNAS license](https://www.pnas.org/lookupto/doi/10.1073/pnas.2020891118/-DCSupplemental).

<sup>1</sup>M.L., W.Z., and Z.H. contributed equally to this paper.

<sup>2</sup>To whom correspondence may be addressed. Email: [baixc15@smu.edu.cn](mailto:baixc15@smu.edu.cn) or [zzp@smu.edu.cn](mailto:zzp@smu.edu.cn).

This article contains supporting information online at <https://www.pnas.org/lookupto/doi/10.1073/pnas.2020891118/-DCSupplemental>.

Published July 23, 2021.

## Results

### Epithelial Tsc1 Ablation Disrupts AJ/TJ Structures and Induces Crohn's Disease- and Psoriasis-Like Phenotypes in Mice.

To investigate the role of mTORC1 in both the small and large intestine, we generated a genetic mouse model, in which Tsc1 was ablated specifically in villi and crypt epithelial cells (*Villin-Cre;TSC1<sup>FL/FL</sup>*, knockout [KO]) (*SI Appendix, Fig. S1A*). As expected, Tsc1 immunostaining was greatly reduced in small intestine sections of *Villin-Cre; TSC1<sup>FL/FL</sup>* mice (*SI Appendix, Fig. S1B*). When compared to control littermates (*TSC1<sup>FL/FL</sup>*), *Villin-Cre; TSC1<sup>FL/FL</sup>* mice showed an increased death rate at ~3 wk. At this time point, *Villin-cre;Tsc1<sup>FL/FL</sup>* mice also experienced significant weight loss (Fig. 1A) and appeared leaner and smaller than control mice (Fig. 1B). They also excreted watery diarrhea. An examination of intestinal tracts from the KO mice revealed a markedly shortened intestinal length (Fig. 1C), increased bleeding (Fig. 1D), and histopathological impairments, such as crypt epithelial degeneration, reductions in goblet cells, and neutrophil infiltration in small intestine and colon sections (Fig. 1E). These phenotypes are commonly found in mice with intestinal barrier dysfunction (28, 29), indicating that Tsc1 ablation disrupts epithelial barriers. To determine how Tsc1 loss affected intestinal epithelium in *Villin-Cre;TSC1<sup>FL/FL</sup>* mice, we analyzed the ultrastructure of cell–cell contacts in KO and control intestinal sections using transmission electron microscopy (TEM). Intercellular spaces at both TJs and AJs were significantly widened in *Villin-Cre;TSC1<sup>FL/FL</sup>* mice, in comparison with control mice. Additionally, TJ shortening was accompanied by AJ lengthening (Fig. 1F), suggesting a role of Tsc1 in AJ and TJ formation. Consistent with the AJ defects, E-cadherin, which directly bridges neighboring epithelial cells and nucleates AJ formation (11), was markedly decreased at cell–cell contacts (Fig. 1G). Similarly, proteins involved in TJ formation, including occludin, claudin 1, and ZO-1, were also reduced at these sites (Fig. 1G). To examine whether Tsc1 was also involved in AJ and TJ assembly at other epithelial tissues, a whole-body Tsc1 KO was induced by treatment with 4-hydroxytamoxifen in mice expressing *Cre-ERT2* fused to floxed *TSC1* under the control of the human ubiquitin C promoter (*Cre-ERT2;TSC1<sup>FL/FL</sup>*) (*SI Appendix, Fig. S1C*). Similar reductions in E-cadherin and ZO-1 levels at cell–cell contacts in colon epithelia (Fig. 1H) and skin (stratum granulosum) (Fig. 1I) were observed in the deletion mice (*SI Appendix, Fig. S1D*). The skin of deletion mice displayed histopathological alterations typical for psoriasis (e.g., thick, extensive cutaneous plaques; epidermal hyperplasia; and parakeratosis) (Fig. 1J). Importantly, these phenotypes of TJ disruption in intestinal and skin epithelia could not be reversed by oral rapamycin treatment, despite a down-regulated mTOR activity, as indicated by dramatically reduced phosphorylation of ribosome protein S6 (S235/236), a widely accepted marker of mTOR activity (*SI Appendix, Fig. S2*). These findings demonstrate that Tsc1 plays a role in AJ/TJ assembly and barrier establishment in the epithelia of multiple organs, likely in an mTOR-independent manner.

**Tsc1 Localizes to Epithelial Junctions.** Tsc1 localizes to the cytoplasm and lysosome surface (30). However, given the effect of Tsc1 on AJs and TJs, we examined Tsc1 localization in the epithelia of human skin and colon samples. Confocal imaging revealed that Tsc1 colocalized with the TJ marker ZO-1 at cell–cell contacts in the epithelia of skin (stratum granulosum) (Fig. 2A) and colon (Fig. 2B), in which TJs play fundamental physiological roles. The colocalization of Tsc1 with TJ marker claudin-1 in skin (Fig. 2C) and colon epithelia (Fig. 2D) was confirmed by another antibody against Tsc1. The specificity of these two antibodies in immunofluorescence staining was further confirmed using intestinal and skin epithelia of the *Cre-ERT2;TSC1<sup>FL/FL</sup>* mice induced for whole-body Tsc1 KO, as well as in Caco-2 cells silenced by Tsc1 short hairpin (shRNA) (*SI Appendix, Fig. S3 A–C*).

To further characterize Tsc1 localization in vivo, skin and intestinal epithelia from C57BL/6J mice were examined using confocal microscopy. Tsc1 was localized at cell–cell contacts of epithelial tissues in the small intestine (Fig. 2E), the colon, and the epidermis (stratum granulosum) (*SI Appendix, Fig. S3D*). Unexpectedly, Tsc2, the partner of Tsc1 in mTORC1 regulation, was not observed at cell–cell contacts in the epithelia of the same tissues. Instead, Tsc2 exhibited a diffused cytoplasmic distribution, without significant colocalization with ZO-1, occludin, and claudin-1, when compared to Tsc1 (Fig. 2F and *SI Appendix, Fig. S3E*). Likewise, while Tsc1 and Tsc2 largely colocalized with each other in Caco-2 cells before the establishment of cell–cell junctions, they exhibited little colocalization in the Caco-2 monolayer, as well as in these epithelial tissues (*SI Appendix, Fig. S4 A–D*). Collectively, these data suggested that Tsc1 may have a Tsc2-independent function at epithelial junctions in vivo.

### Tsc1 Translocates from the Cytoplasm to Junctional Membranes When Adjacent Cells Establish Contact.

Dynamic changes in Tsc1 and Tsc2 localization were traced during the formation of intestine-like Caco-2 monolayers (31, 32). Before forming monolayers, Tsc1 was observed mainly in the cytoplasm with a punctate pattern, consistent with previous observations (33). However, after cells formed monolayers (11 d after seeding), Tsc1 was localized primarily to cell–cell junctions, colocalizing with  $\beta$ -catenin, occludin, and claudin-1 (Fig. 3A), as revealed by confocal imaging. This junctional localization of Tsc1 in Caco-2 cells was also confirmed by another Tsc1 antibody (*SI Appendix, Fig. S5*). However, Tsc2 was mainly localized to the cytoplasm of Caco-2 cells, regardless of monolayer formation status (Fig. 3B). Ultrastructural analyses using immunoelectron microscopy further revealed that Tsc1 moved from lysosome-like vesicles to both AJs and TJs at junctional membranes when cells established contact (Fig. 3C).

Interestingly, Tsc1 protein expression was significantly enhanced after monolayer formation, suggesting that an up-regulation of Tsc1 is required to establish cell–cell contact (Fig. 3D). This increased protein level of Tsc1 may be attributed to increased synthesis or stability, since no significant alteration in its messenger RNA (mRNA) expression was observed (Fig. 3E). In contrast, Tsc2 protein expression was markedly decreased after monolayer formation (Fig. 3D), correlated with a dramatic reduction of Tsc1 binding to Tsc2 (Fig. 3F), indicating that after Tsc1 translocation to junctional membranes, the lack of Tsc1 binding led to Tsc2 destabilization and degradation. However, the reduction in Tsc2 was not accompanied by increased mTORC1 activity. Instead, a dramatic reduction in mTORC1 activity was observed after monolayer formation, as evident from phosphorylation levels of the ribosome protein S6 (S235/236) (Fig. 3D). This decrease in mTORC1 activity may have been caused by reduced PI-3K/Akt activity, as shown by phosphorylation of Akt (T308) (Fig. 3D). Consistently, we observed a dramatic increase in the level of Tsc1 in the membrane fraction (plasma membranes and organelle membranes), concomitant with its marked decrease in the cytosol fraction, as revealed by fractionation analysis (Fig. 3D). In contrast, Tsc2 was barely detectable in the membrane fraction before or after monolayer formation (Fig. 3D).

To confirm whether there exists a Tsc2-independent population of Tsc1, lysates from Caco-2 cells before or after monolayer formation were subjected to sucrose density gradient assay. Consistent with results obtained by membrane fractionation, a Tsc2-free population of Tsc1 appeared in low-density fractions (fraction 3 to 5) after monolayer formation (Fig. 3G). Consistently, similar Tsc2-independent Tsc1 pools (fraction 3 to 5) were found in cell extracts from both intestinal and skin epithelia of C57BL/6J mice (Fig. 3H). Collectively, these results suggest that a proportion of Tsc1 is translocated to the junctional membranes, independent of Tsc2 when epithelial monolayer is established.

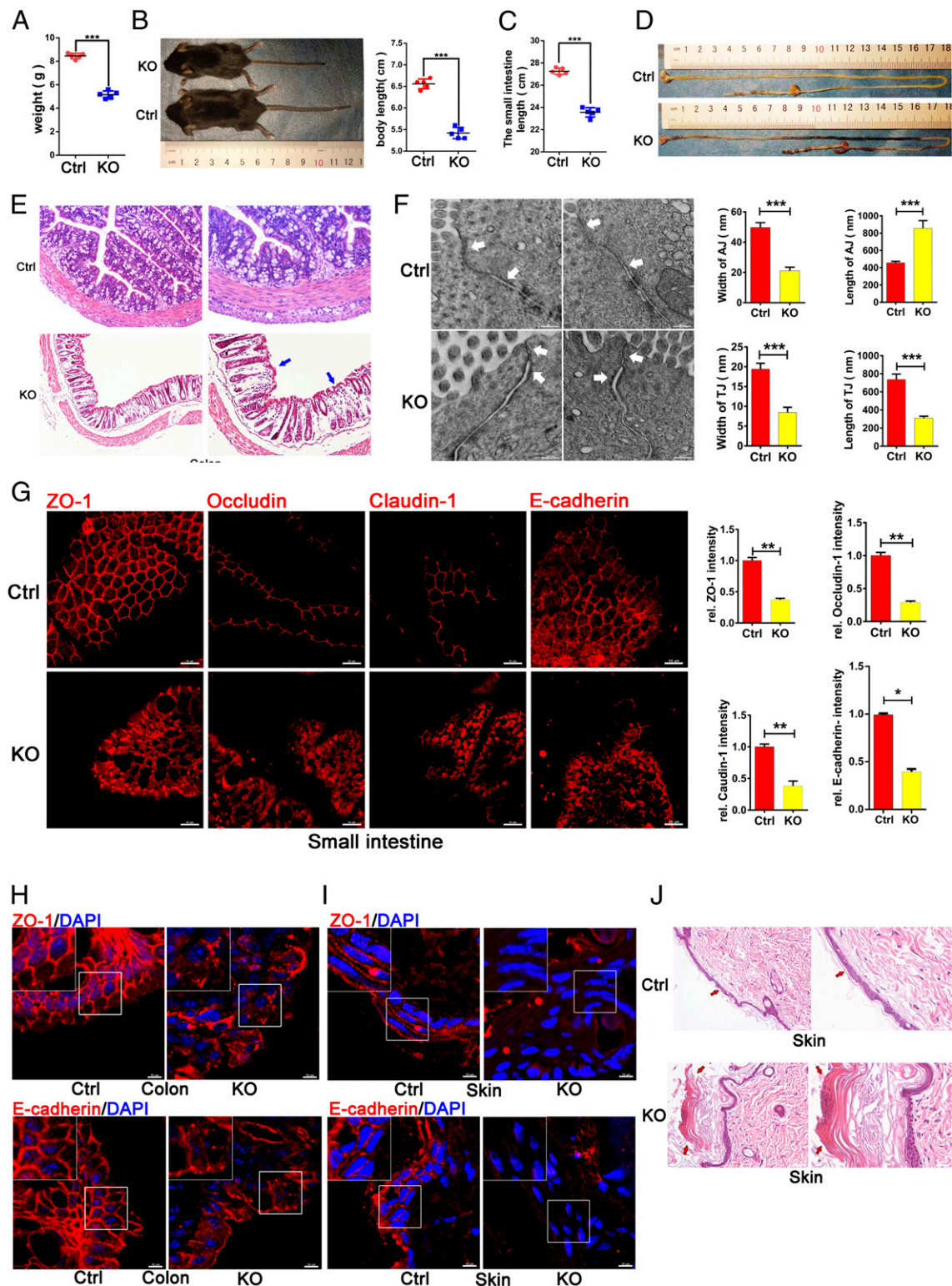


**Fig. 1.** *TSC1* ablation in epithelia results in barrier dysfunction and disorganization of AJs/TJs in mice. Control (Ctrl) mice or mice with *TSC1* ablation in intestinal villi and crypt epithelial cells (*Villin-Cre;TSC1<sup>FL/FL</sup>* [KO]; *SI Appendix, Fig. S1*) were evaluated for body weight and length (A), general nutrition (B), intestinal length (C), and intestinal bleeding and swelling (D). \*\*\* $P < 0.0001$  ( $n = 6$ ). (E) Hematoxylin–eosin (HE) staining of small intestinal sections from indicated mice. \*\*\* $P < 0.0001$  ( $n = 6$ ). (F) The ultrastructure of cell–cell contacts in intestinal sections from Ctrl and KO mice were analyzed by TEM. TJs and AJs are indicated by white arrows (Left), with their width and length quantitated (Right). (Scale bar, 20 nm.) Error bars denote the means  $\pm$  SEM \*\*\* $P < 0.0001$  ( $n = 6$ ). (Left) Small intestinal (G) and colon sections (H) from these mice were analyzed for the indicated AJ and TJ markers by fluorescence confocal microscopy. (Scale bar, 10  $\mu$ m.) (Right) The relative intensity of the immunofluorescence signals at cell–cell contacts were analyzed using ImageJ software. Data are expressed as ratios of normalized junctional fluorescence intensities (against DAPI) per cell. Error bars denote the means  $\pm$  SEM, \*\*\* $P < 0.0001$ , \*\* $P < 0.01$ , and \* $P < 0.05$  ( $n = 6$ ). *Cre-ERT2;TSC1<sup>FL/FL</sup>* mice were treated with 4-hydroxytamoxifen to induce whole-body *Tsc1* KO. (I) Tissue sections from the skin were analyzed for  $\beta$ -catenin and ZO-1 expression and localization using confocal microscopy. (Scale bar, 10  $\mu$ m.) (J) HE staining of colon and skin sections from indicated mice.

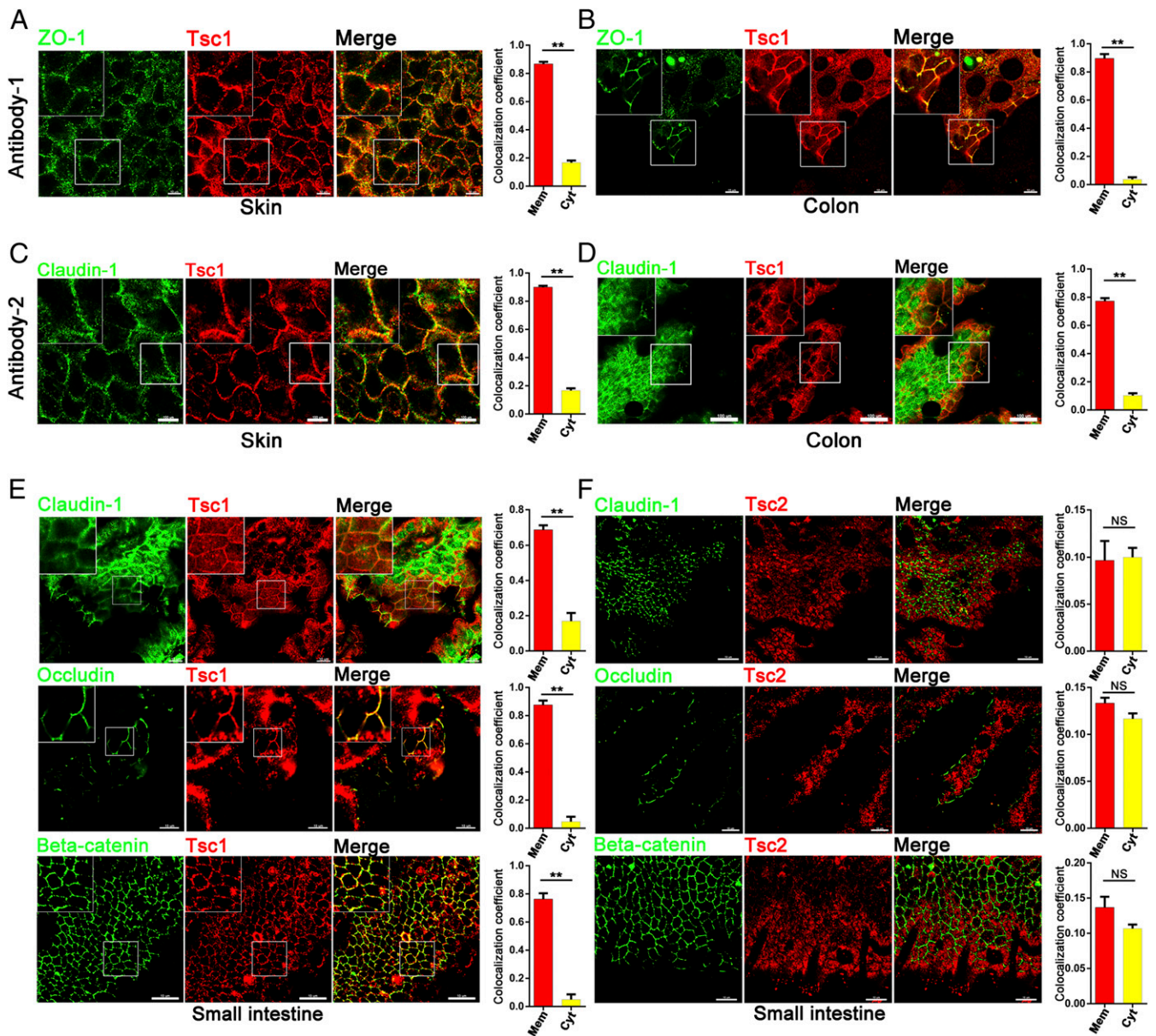


**Fig. 2.** Tsc1, but not Tsc2, is localized to epithelial junctions in humans and mice. The subcellular localization of Tsc1 and TJ ZO-1 in human skin (A) and colon (B) specimens was analyzed by fluorescent confocal microscopy. The localization of Tsc1 in human skin (C) and colon (D) specimens was analyzed the same way using another primary Tsc1 antibody. The subcellular localization of Tsc1 and Tsc2 (F), with indicated AJ/TJ markers in small intestinal sections from wild-type C57B/6 mice, were analyzed by fluorescent confocal microscopy. (Scale bar, 10  $\mu$ m.) (A–F, Right) Manders' coefficient was used to calculate the colocalization of Tsc1 and Tsc2 with indicated AJ/TJ markers at membrane (Mem) or cytosol (Cyt). Error bars denote the means  $\pm$  SEM, \*\*\* $P$  < 0.0001, \*\* $P$  < 0.01, and \* $P$  < 0.05 ( $n$  = 6). NS, not significant. Enlarged *Insets* are shown at the upper left corner of A–E.

To verify that the junctional localization of Tsc1 was mediated through AJ and TJ associations, we performed a liquid chromatography–tandem mass spectrometry (LC-MS/MS) analysis of the interacting proteins of ZO-1 (gene name TJP1), a key scaffold TJ protein, before and after monolayer formation in Caco-2 cells. Analysis of ZO-1–interacting proteins specific for Caco-2 monolayer confirmed the association of ZO-1 with other AJ/TJ proteins and Tsc1 (SI Appendix, Fig. S6A). Increased ZO-1 interaction with Tsc1, after Caco-2 monolayer formation, were further confirmed by immunoprecipitation (IP) analysis (SI Appendix, Fig. S6B). These results indicated a physical association of Tsc1 with TJs.

**Epithelial Tsc1 Maintains TJ Barrier Function In Vitro.** TJs prevent the flux of most hydrophilic solutes, as well as seal the paracellular or

shunt pathway between cells (4). To determine the role of Tsc1 in this TJ function, we analyzed transepithelial electrical resistance (TER) and the paracellular permeability of Tsc1-depleted cells. Depletion of Tsc1 by shRNA in Caco-2 cells resulted in significantly reduced TER (Fig. 4A, Left), as well as a marked increase in paracellular large-molecule permeability, as demonstrated by the transwell FITC-dextran assay (Fig. 4A, Middle). The defect in the paracellular permeability of Tsc1 depletion cells was not rescued by rapamycin treatment (Fig. 4B, Left and Middle), suggesting that the role of Tsc1 in TJ function was mTORC1 independent. In contrast, Tsc2 depletion had little effect on either TER or paracellular permeability (Fig. 4C, Left and Middle), further suggesting that Tsc1 controls TJ function, independent of Tsc2. The effects of Tsc1 and Tsc2 knockdown,

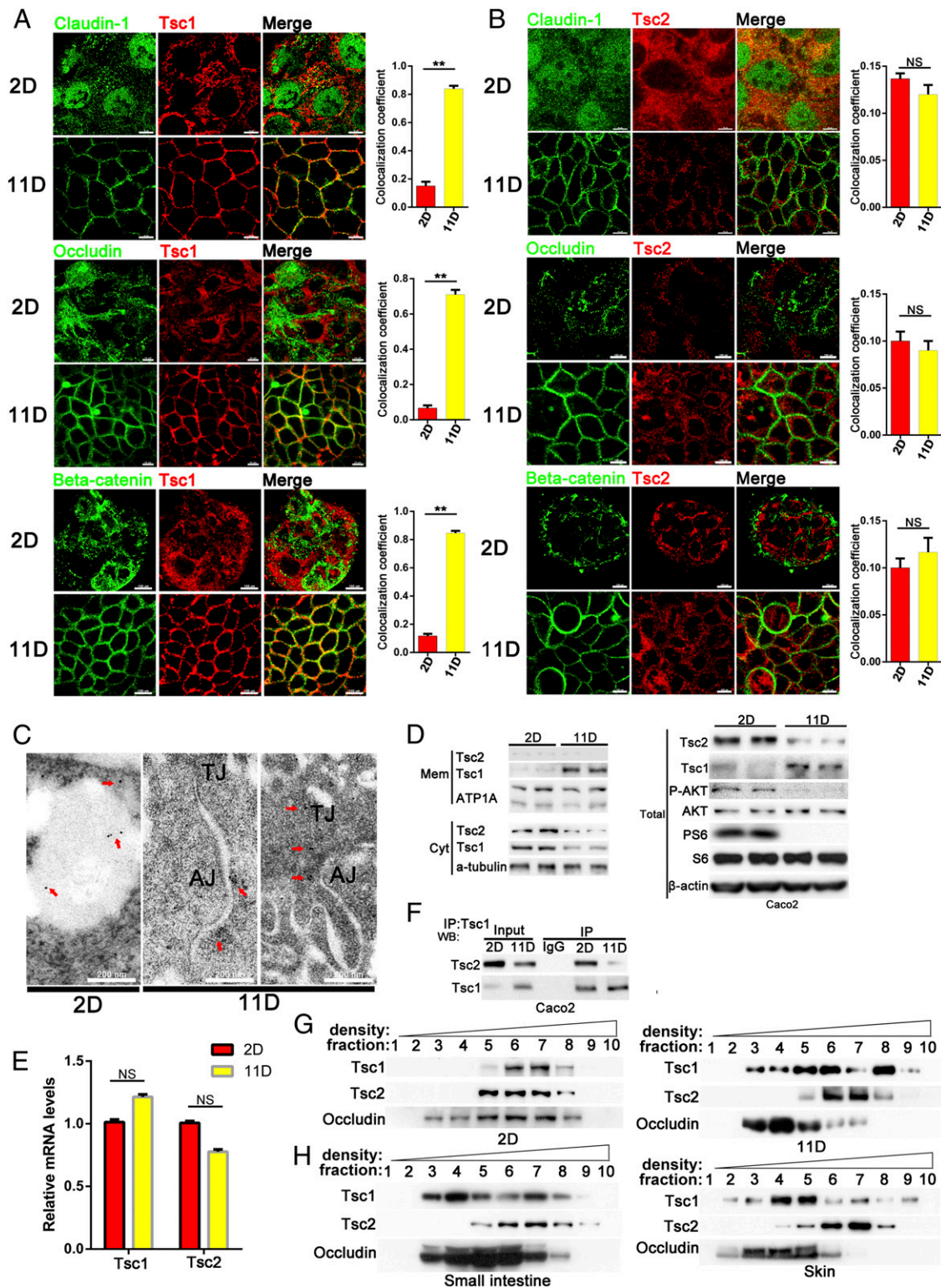


**Fig. 3.** Tsc1 translocates from the cytoplasm to junctional membranes when adjacent cells establish contact. (A) The subcellular localization of Tsc1 with indicated AJ/TJ markers before (2 d after seeding) or after Caco-2 monolayer formation (11 d after seeding) was analyzed by fluorescent confocal microscopy. (B) The subcellular localization of Tsc2 with the indicated TJ markers before and after Caco-2 monolayer formation was analyzed as in A. (A and B, Right) Manders' coefficient was used to calculate the colocalization of Tsc1 and Tsc2 with indicated AJ/TJ markers. Error bars denote the means  $\pm$  SEM,  $**P < 0.01$  ( $n = 3$ ). NS, not significant. (C) Tsc1 localization at Caco-2 cell-cell contacts before and after monolayer formation was examined by immunoelectron microscopy using immunogold labeling. (D) Whole-cell (Total), cytoplasmic (Cyt) and membrane (Mem) fraction proteins from Caco-2 cells, before and after monolayer formation, were extracted and analyzed by Western blotting (WB). (E) Total RNA of the Caco-2 cells before and after monolayer formation were extracted and analyzed for Tsc1 mRNA expression using RT-qPCR. (F) Caco-2 cells before or after monolayer formation were lysed. The cell lysates were precipitated with anti-Tsc1 antibody. The levels of Tsc2 coprecipitated with Tsc1 were examined by WB. Lysates of Caco-2 cells before and after monolayer formation (G), of small intestine (H, Left), or of skin epithelia (H, Right) were subjected to sucrose density fractionation, followed by fractions 1 to 10 (from top to bottom) analyzed for the indicated protein by WB.

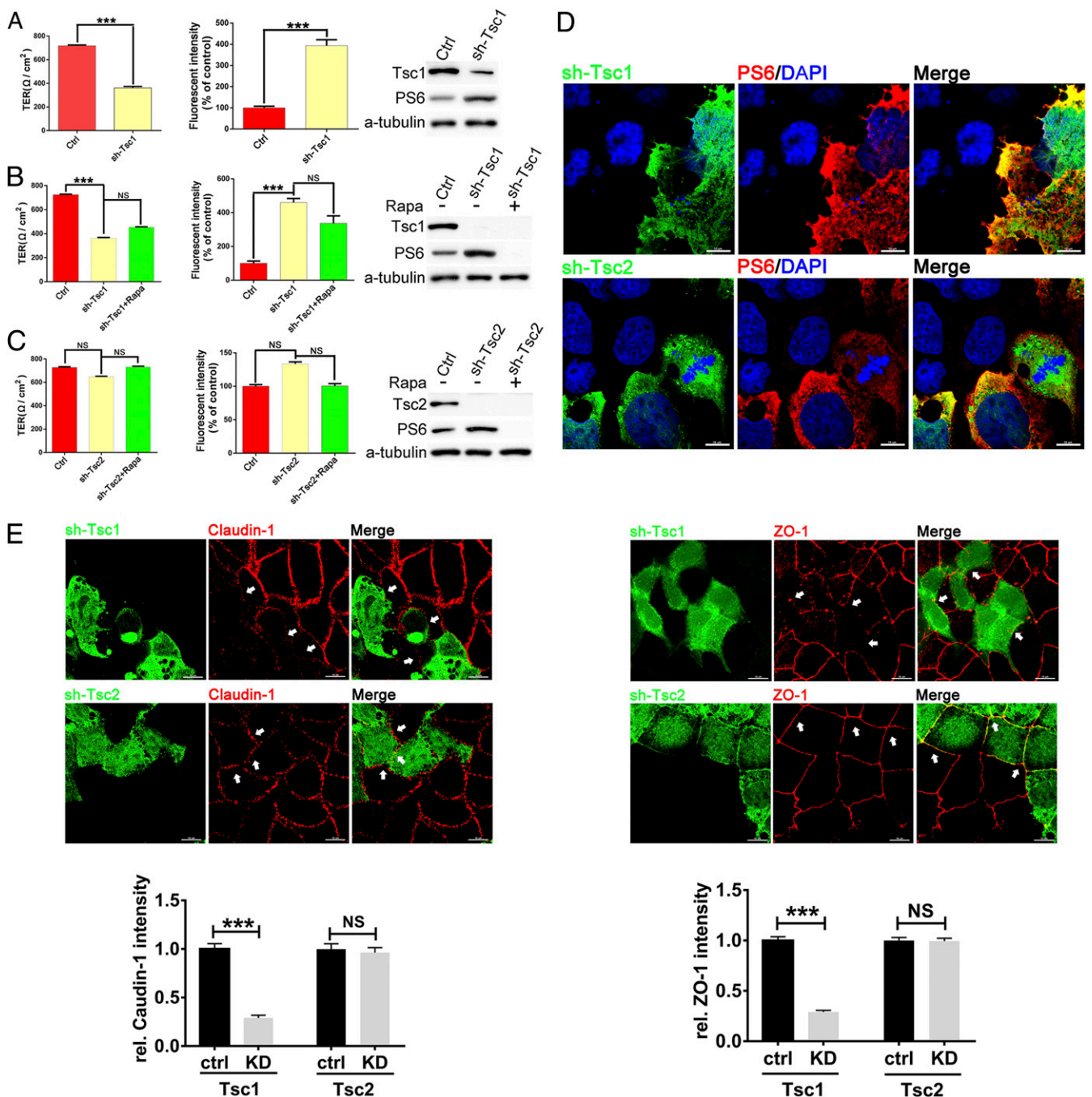


**Fig. 4.** Depletion of Tsc1 impairs epithelial TJ barrier function in vitro. Control (Ctrl) or Tsc1 shRNA was transfected into Caco-2 cells using a lentiviral vector. (A) After seeding for 11 d (monolayer), transmembrane electric resistance (TER) (Left) or flux of paracellular 10 kDa FITC-dextran (Middle) was measured, respectively. (B) The effects of rapamycin on Caco-2 cells stably transfected with Tsc1 shRNA were also assayed using TER (Left) or paracellular flux of 10 kDa FITC-dextran (Middle). \*\*\* $P < 0.0001$  ( $n \geq 3$ ). (C) Ctrl or Tsc2 shRNA was transfected into Caco-2 cells and analyzed as in A. NS, not significant. Parallel wells of Caco-2 cells treated as in A–C were analyzed for phosphorylation of ribosome protein S6 to evaluate the efficiency of Tsc1/2 depletion or rapamycin treatment (A–C, Right). Caco-2 cells were stably transfected with either Tsc1 (or Tsc2) shRNA encoded by a GFP-lentiviral vector or Ctrl shRNA encoded by the same lentiviral vector lacking GFP. These cells were mixed and cocultured until monolayer formation, with phosphorylation of ribosome protein S6 at S235/236 before monolayer formation (D) and TJ marker expression after monolayer formation (E) analyzed by fluorescence confocal microscopy (Upper) and the immunofluorescence signals at cell–cell contacts quantitated by ImageJ software (Lower). Data are presented as normalized junctional fluorescence intensity (against DAPI) per cell. Error bars denote the means  $\pm$  SEM, \*\*\* $P < 0.0001$  ( $n = 100$ ). NS, not significant. (Scale bar, 10  $\mu$ m.) ctrl, control; KD, knockdown.

as well as that of rapamycin treatment, on mTORC1 activity were confirmed by assay of S6 phosphorylation (Fig. 4 A–C, Right). To further determine the effects of Tsc1 on cell adhesion, Caco-2 cells were stably transfected with either Tsc1 shRNA encoded by a GFP-lentiviral vector or control shRNA encoded

by the same lentiviral vector lacking GFP. To observe the effect of Tsc1 depletion on TJ protein expression within the same microscopic field of view (34), the cells were mixed in a 1:1 ratio and cocultured until monolayer formation. The knockdown efficiency of Tsc1 was indicated by increased mTORC1 activity, as

reflected by enhanced S6 phosphorylation in FITC-labeled cells before cell contact was established (Fig. 4D). After cells established contact, those transfected with Tsc1 shRNA exhibited reduced levels of ZO-1 and claudin 1 at cell–cell contacts, in comparison with those cells in which Tsc1 was not inhibited by shRNA (Fig. 4E). In contrast, Tsc2-depleted cells were examined in the same way; no defect was observed in junctional protein distribution (Fig. 4E).

**Tsc1 Retains  $\beta$ -catenin and ZO-1 at AJ/TJ by Myo6-Dependent Perijunctional F-actin Stabilization.** To determine the mechanism underlying the role of Tsc1 in AJ/TJ formation, we examined Tsc1-interacting proteins before and after Caco-2 monolayer formation by Coomassie blue staining (SI Appendix, Fig. S7A). After confirming immunoprecipitated TSC1 and TBC1D7, a third subunit of TSC complex (35) by Western blotting (SI Appendix, Fig. S7B), these proteins were then analyzed using an LC-MS/MS approach. Evaluation of Tsc1-interacting proteins specific for Caco-2 monolayer revealed that Tsc1 became associated with AJ/TJ proteins upon epithelial cell–cell contact (SI Appendix, Fig. S7C). These junctional proteins included  $\beta$ -catenin (*CTNBN1*), a critical scaffold protein bridging intercellular junctions and the perijunctional cytoskeleton (11), and ZO-1, which interacts with claudin-1 (12). Additionally, Tsc1 became associated with Myo6, an unconventional myosin that binds  $\beta$ -catenin in vitro and is required to maintain perijunctional actin cytoskeleton connections with both AJs and TJs (36, 37) (SI Appendix, Fig. S7C). The enhanced interaction of Tsc1 with Myo6,  $\beta$ -catenin, and ZO-1 after monolayer formation was verified by co-IP assays (Fig. 5A). In line with the findings, only a small amount of Myo6 cofractionated with Tsc1 (in fractions 5 to 7) before monolayer formation. However, the amount of Myo6 cofractionated with Tsc1 was markedly increased (in fractions 3 to 5) after monolayer formation (Fig. 5B). Likewise, a significant portion of Myo6 was cofractionated with Tsc1 in extracts from intestine epithelia and epidermis (Fig. 5C). These data collectively suggest that the colocalization of Tsc1 and Myo6 is strengthened to enhance their interaction after epithelial cells establish cell–cell junctions.

To determine if Tsc1 controlled AJ and TJ through Myo6, we examined how Tsc1 affected Myo6 binding with  $\beta$ -catenin and ZO-1. We observed that Tsc1 depletion did not affect  $\beta$ -catenin and Myo6 protein levels (Fig. 5D). However, Tsc1 depletion greatly reduced association of Myo6 with both  $\beta$ -catenin and ZO-1. In contrast, Tsc2 depletion had little effect on the association (Fig. 5E). Conversely, when Myo6 was depleted, the association of Tsc1 with  $\beta$ -catenin and ZO-1 was also dramatically reduced (Fig. 5F). Consistent with the reduced association of  $\beta$ -catenin with Myo6 in Tsc1-depleted cells, the localization of both  $\beta$ -catenin and Myo6 at cell–cell contacts was markedly reduced after monolayer formation. In Myo6-depleted cells, Tsc1 and  $\beta$ -catenin displayed similar distribution defects at intercellular contacts (Fig. 5G). These data suggested that Tsc1 and Myo6 were mutually dependent in their association with  $\beta$ -catenin and ZO-1 and that the association with Tsc1 and Myo6 was essential for correct  $\beta$ -catenin and ZO-1 localization at cell–cell contacts. Consistent with these in vitro data, a marked reduction in  $\beta$ -catenin localization at cell–cell contacts was observed in small intestinal sections of *Villin-Cre;TSC1<sup>FL/FL</sup>* mice, when compared to control mice (Fig. 5H), suggesting that Tsc1 recruits or retains  $\beta$ -catenin at cell–cell contacts. Since Myo6 is required to stabilize the perijunctional actin cytoskeleton (37), the effect of Tsc1 depletion on perijunctional F-actin was analyzed by confocal microscopy. As expected, both Tsc1 and Myo6 deficiency disrupted perijunctional F-actin organization (Fig. 5I). Taken together, these results suggested that Tsc1 acts together with Myo6 to retain ZO-1 and  $\beta$ -catenin at intercellular contacts and, consequently, stabilizes perijunctional actin cytoskeleton.

**Tsc1 Directly Binds to Myo6.** To verify whether Tsc1 directly bound to  $\beta$ -catenin and Myo6, the GST-Tsc1 cassette was cloned into a mammalian-expressing vector, expressed and purified from human embryonic kidney 293 lysates, and incubated with  $\beta$ -catenin or Myo6 translated using the TNT in vitro translation system. GST-Tsc1 bound to Myo6 but not  $\beta$ -catenin (Fig. 6A), suggesting that Tsc1 does not bind  $\beta$ -catenin directly but may associate with  $\beta$ -catenin via Myo6. To identify the Tsc1 regions responsible for binding with Myo6, various Tsc1 truncation mutants were constructed and expressed as GST-fusion proteins. Tsc1 contains a Tsc2-binding domain (BD) (amino acids 302 to 430) and a short hydrophobic sequence (HS) predicted to be a potential transmembrane domain (38, 39). We observed that Tsc1 truncation mutants lacking the Tsc2-BD (TSC2 BD mutant) were unable to bind Myo6 (Fig. 6B), suggesting that this domain in Tsc1 mediates its interaction with Myo6. This raises a possibility that Myo6 competes with Tsc2 for the binding of Tsc1. Consistent with this notion, an addition of Myo6 into a binding reaction containing Tsc1 and Tsc2 reduced their binding to each other (Fig. 6C). In Caco-2 cells, like the Tsc1 HS mutant, the Tsc2-BD mutant failed to translocate to intercellular contacts after monolayer formation (Fig. 6D). This observation suggests that Tsc1 binding to Myo6 is required for Tsc1 localization at junctional membranes.

Several pathologic mutations of *TSC1* identified in TSC patients, including 593 to 595del ACT;N198\_F199delinsI (39) and 1122delCA;Q301fs-302x (40), result in the production of Tsc1 protein unable to bind Tsc2. Interestingly, these two mutants were also unable to bind to Myo6, as revealed by the GST pull-down assay (SI Appendix, Fig. S8). These results raise the possibility that the pathogenic mutations of Tsc1 may affect formation of TJ.

#### Epithelial Junctional Tsc1 Is Reduced in TJ-Related Human Diseases.

As Tsc1-deficient mice exhibited symptoms associated with TJ-related diseases, we examined whether Tsc1 deficiency is associated with TJ-related diseases in human. Tsc1 expression at the mRNA level was analyzed in TJ-related diseases using data from Gene Expression Omnibus. The analysis revealed that Tsc1 mRNA was significantly reduced in Crohn's disease and psoriasis (Fig. 7A). In addition, Tsc1 mRNA was modestly decreased in nonlesional AD but markedly decreased in lesional AD (Fig. 7A). Epithelial tissue sections from patients with these diseases and control subjects were examined to verify the down-regulation of Tsc1 protein in epithelia of these patients. When the expression of Tsc1 in the epithelia of the colon from patients with Crohn's disease was compared with those from healthy subjects, a marked decrease was observed in the patient samples in comparison with control samples (SI Appendix, Fig. S9A). Confocal imaging further showed the drastic reduction of Tsc1 at the epithelial junctional membrane in the patient samples, concomitant with a significant reduction in the TJ marker ZO-1 (Fig. 7B). A similar reduction of Tsc1 was observed in the skin samples of patients with AD or psoriasis (SI Appendix, Fig. S9C). The levels of Tsc1 and ZO-1 at the epithelial junctional membranes of the patient samples were also reduced (Fig. 7C). In all the tissues samples examined in Fig. 7B and C, a compromised epithelial integrity was evident (SI Appendix, Fig. S9B and D). These results suggest that a reduced level of junctional Tsc1 is associated with impaired epithelial structures in human epithelial tissues.

Taken together, our results suggest that Tsc1 plays a critical role in AJ/TJ formation, independent of its role in mTORC1 regulation. At the junctional membrane during epithelial AJ/TJ formation, Tsc1, in complex with Myo6, stabilizes perijunctional actin and  $\beta$ -catenin/ZO-1 associations. Conversely, the loss of junctional Tsc1 results in disorganization of perijunctional actin and AJ/TJ.

#### Discussion

Tsc1 has long been known for its role in Tsc2-dependent regulation of mTORC1. Its inactivation causes hyperactive mTORC1

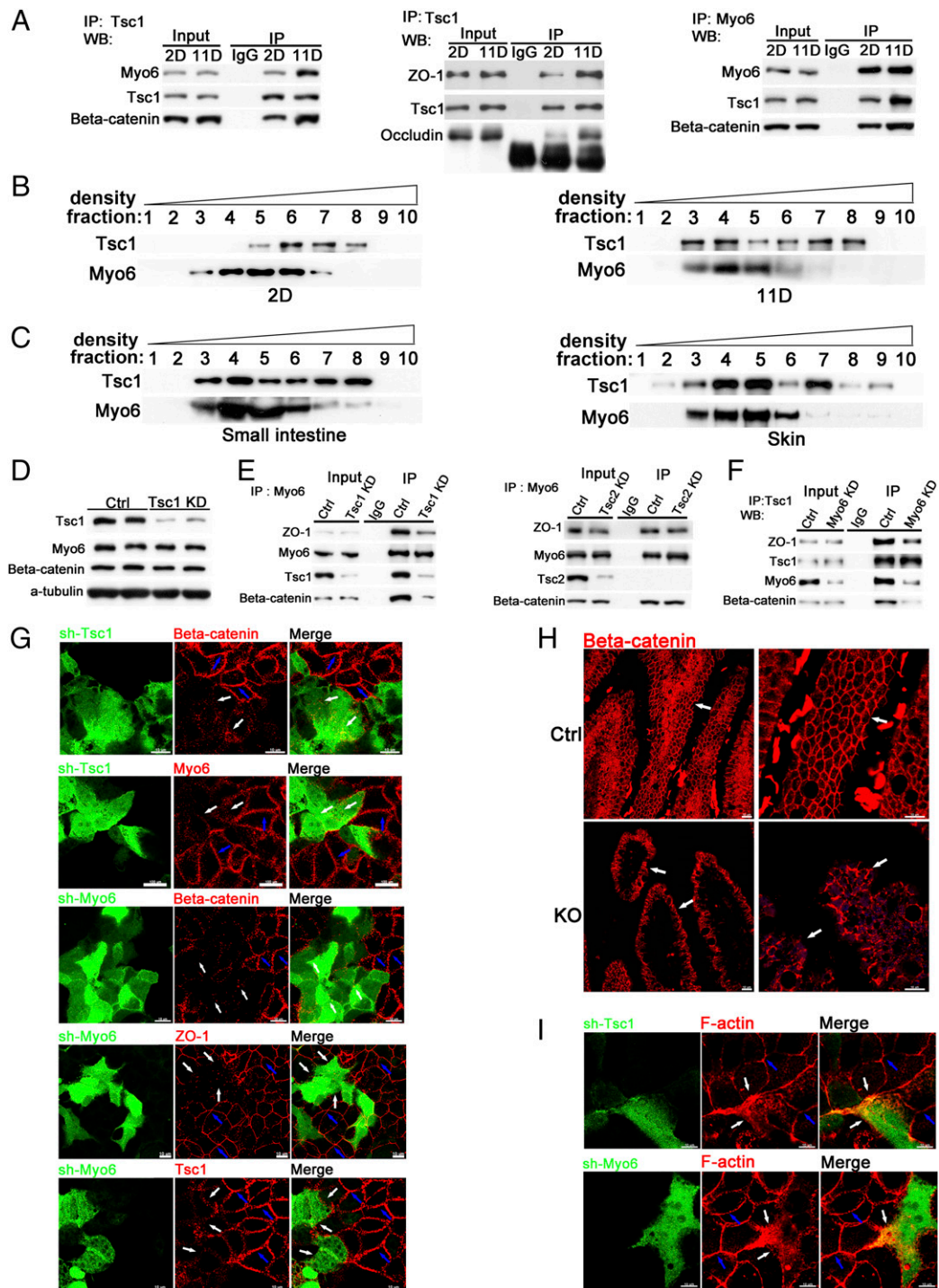


**Fig. 5.** Tsc1 binds Myo6 to retain  $\beta$ -catenin and ZO-1 at AJs/TJs. (A) Caco-2 cells were seeded and cultured for 2 d (before monolayer formation) or 11 d (monolayer formed). The binding of Tsc1 to  $\beta$ -catenin, ZO-1, and Myo6, before and after Caco-2 monolayer formation was analyzed by reciprocal immunoprecipitation. Lysates of Caco-2 cells before and after monolayer formation (B) or that of colon or skin epithelia (C) were subjected to sucrose density fractionation, followed by fractions 1 to 10 (from top to bottom) analyzed for Tsc1 and Myo6 by Western blotting (WB). (D)  $\beta$ -catenin and Myo6 expression in Caco-2 cells, upon Tsc1 depletion, was assayed by WB. (E) The association of  $\beta$ -catenin with Myo6 in cells depleted of Tsc1 or Tsc2 was assayed by immunoprecipitation. (F) The association of Tsc1 with  $\beta$ -catenin or ZO-1 in cells depleted of Myo6 was analyzed as for E. (G) Caco-2 cells were stably transfected with either Tsc1 (or Myo6) shRNA encoded by a GFP-lentiviral vector or Ctrl shRNA encoded by the same lentiviral vector lacking GFP. These cells were cocultured until monolayer formation. ZO-1 and  $\beta$ -catenin in Tsc1-depleted cells, or  $\beta$ -catenin, and Tsc1 localization in Myo6-depleted cells was assayed by confocal microscopy. (Scale bar, 10  $\mu$ m.) (H)  $\beta$ -catenin localization in small intestinal sections of Ctrl and Villin-cre;Tsc1<sup>FL/FL</sup> mice was analyzed by fluorescent confocal microscopy. (Scale bar, 10  $\mu$ m.) (I) F-actin distribution in Tsc1- or Myo6-depleted cells was examined by confocal microscopy after staining with phalloidin. While white arrows were used to indicate impaired AJs/TJs, blue arrows were used to indicate the normal AJs/TJs. KD, knockdown.

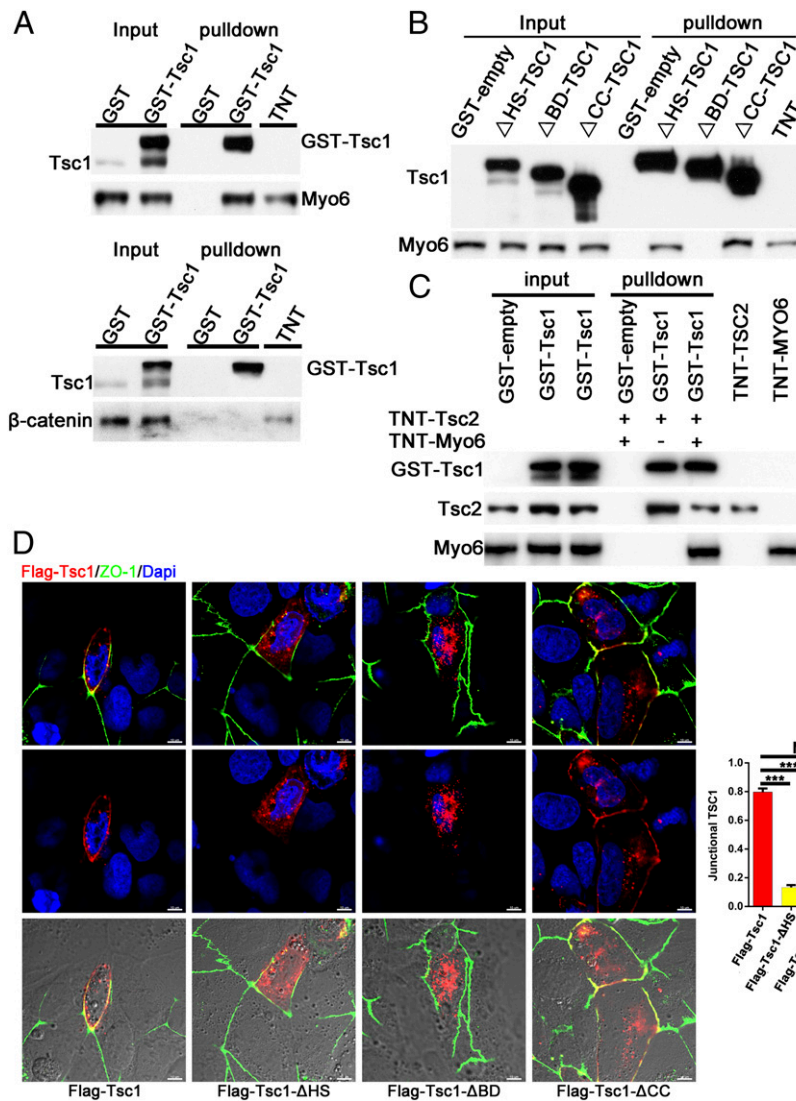


**Fig. 6.** Tsc1 directly interacts with Myo6 through its Tsc2 BD sequence. GST-tagged wild-type (A) and mutant (B) Tsc1 proteins were expressed and purified from human embryonic kidney 293 cells and incubated with recombinant  $\beta$ -catenin or Myo6 translated in vitro. TNT is the input for proteins translated in vitro. The coprecipitated proteins were analyzed by Western blotting. (C) GST-Tsc1 purified as in A was incubated with Tsc2 translated in vitro (TNT-Tsc2) in the presence or absence of TNT-Myo6 (1:1 ratio), with coprecipitated proteins analyzed by Western blotting. (D) Localization of Flag-tagged Tsc1 mutants in Caco-2 monolayers was analyzed by fluorescent confocal microscopy. Representative images from three independent experiments were shown in the left panel, and junctional Tsc1 was calculated as colocalization of Tsc1 with TJ marker ZO-1 (Manders' coefficient) in the right panel. Error bars denote the means  $\pm$  SEM,  $**P < 0.01$  ( $n = 3$ ). NS, not significant.

and abnormal cell proliferation, which underlies the pathogenesis of TSC syndrome (41). In this study, we show that Tsc1 has a previously unknown yet critical function in controlling cell-cell adhesion. This unique function is essential for AJ/TJ formation and independent of Tsc2 and mTORC1. In Tsc1-deficient epithelial cells, the integrity of both AJs and TJs at the junctional membrane is largely compromised, with the disruption of perijunctional actin organization. In mice, Tsc1 depletion recapitulated conditions characteristic of TJ-related diseases. Our findings demonstrate that Tsc1 plays a critical role in maintaining epithelia barrier functions and that its down-regulation is associated with TJ-related human diseases.

The role of Tsc1 in cell adhesion requires Myo6, an unconventional myosin. Unlike other myosins, Myo6 is the only known motor that moves toward the minus ends of actin filaments (42, 43). Since the plus ends of actin filaments are oriented toward the plasma membrane, Myo6 either carries its cargos inwards along

actin filaments or, when tethered and unable to move freely, pushes the actin filaments outwards via a protrusive force generated by its motor activity (36, 44). At cell-cell contacts, Myo6 interacts with vinculin and  $\beta$ -catenin and anchors actin filaments to E-cadherin, hence stabilizing AJs. In epithelial cells, the loss of Myo6 disrupts perijunctional actin and reduces TJ markers at cell-cell contacts (37, 45). These phenotypes are reminiscent of our observations in Tsc1-depleted cells, suggesting that Tsc1 and Myo6 function through the same mechanism to maintain AJ stability. In support of this view, we observed that Tsc1 interacted directly with Myo6 (Fig. 6A). In addition, the junctional membrane distribution of Myo6 and Tsc1 is interdependent; in the absence of either one, the other is lost. These observations suggest that these two proteins function together to stabilize AJs.

While Tsc1 associates with  $\beta$ -catenin in cells (Fig. 5A), it does not bind directly with  $\beta$ -catenin (Fig. 6A). In this regard, it is unlikely that Tsc1 is directly involved in tethering actin filaments

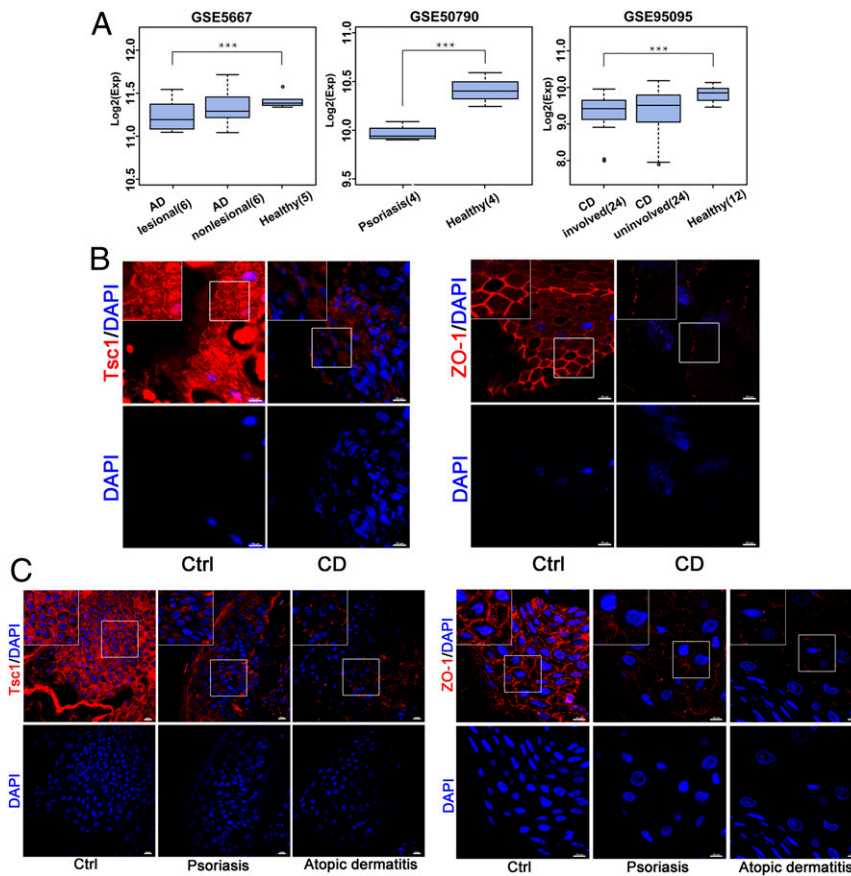


**Fig. 7.** Junctional Tsc1 expression is markedly reduced in patients with TJ-related diseases. (A) Tsc1 mRNA expression analysis of Crohn's disease (CD), AD, and psoriasis human samples in the Gene Expression Omnibus database. Statistic results shown in the box graph were obtained by two-tailed t test or one-way ANOVA with multiple comparisons, followed by Bonferroni's post hoc test for significance.  $***P < 0.001$  (with cases in each group shown in the figure). Error bars represent mean values  $\pm$  SEM. The expression of the Tsc1 (Left) or TJ marker ZO-1 (Right) in colon sections of control (Ctrl) subjects or patients with CD (B), or skin sections of Ctrl subjects or patients with psoriasis or AD (C), was examined by fluorescence confocal microscopy. Representative images are shown. For non-CD Ctrl subjects,  $n = 10$ ; for patients with CD,  $n = 12$ ; for AD and psoriasis healthy subjects,  $n = 20$ ; for patients with psoriasis,  $n = 10$ ; and for patients with AD,  $n = 6$ . (Scale bar, 10  $\mu$ m.) Enlarged Insets are shown at the upper left corner of B and C.

to AJ, as Myo6 is. Thus, it is possible that binding with Tsc1 prevents Myo6 from processive stepping along actin filaments, consequently locking it onto actin filaments to stabilize their connections with AJs. Consistent with this notion, we found that Tsc1 depletion abrogated perijunctional actin distribution (Fig. 5I).

Despite the role of Tsc1 in AJ stability, the major impact of Tsc1 deficiency on the barrier functions of epithelia is caused by defects in TJs. Depletion of Tsc1 results in the loss of junctional membrane distribution of key TJ components, including claudin and ZO-1 (Fig. 4E). In addition, perijunctional actin filaments were also disrupted (Fig. 5I). The effects of Tsc1 on TJ can be direct, through its association with ZO-1, or indirect, through its role in AJ formation. A previous study showed that AJ formation brought the plasma membranes of adjacent cells into close proximity and altered membrane lipid composition, thus allowing claudin retention in the plasma membrane for subsequent TJ formation (8). In this regard, AJ formation and stabilization are essential for TJ assembly, whereas disrupted AJs due to Tsc1 loss hinders TJ assembly. In supporting this notion, mice, with *TSC1* ablated in intestinal epithelia, exhibited prominent shortening of TJs and concomitant AJ lengthening (Fig. 1F), indicating inefficient TJ formation from dysfunctional AJs. However, the physical association of Tsc1 with ZO-1 (Fig. 5A and SI Appendix, Fig. S6) also suggests that Tsc1 may play a direct role in controlling TJ stability, presumably through its involvement in

tethering actin filaments to ZO-1. Therefore, the effects of Tsc1 on TJ are likely to be mediated by its role in AJ and TJ stability.

Previous studies have shown that Tsc1 localizes primarily to cytoplasmic vesicles (33), such as lysosomes (30). Consistent with this observation, we observed in epithelial cells that Tsc1 was present in vesicular structures in the cytoplasm and associated with lysosomal proteins, such as LAMP-1 and LAMP-2, before cells establish contacts with each other. However, upon cell-cell contact, Tsc1 migrated to junctional membranes, where it associated with both AJs and TJs (Fig. 3A). This redistribution is likely to be mediated by a Myo6-dependent mechanism; since we observed that in Myo6-depleted cells, the junctional distribution of Tsc1 was diminished (Fig. 5G). However, it remains unclear how Myo6 controls the junctional distribution of Tsc1. Since Myo6 moves inward along actin filaments, it is unlikely that Tsc1 is a cargo of Myo6. It is possible that Myo6 is required for Tsc1 retention at junctional membranes. Myo6 binds to the same Tsc1 region as Tsc2. Therefore, Myo6 and Tsc2 binding are expected to be mutually exclusive, further suggesting that the role of Tsc1 in cell adhesion is independent of Tsc2. When cells establish contacts, the translocation of Tsc1 to junctional membranes results in reduced Tsc2 levels (Fig. 3D), likely due to Tsc2 instability in the absence of Tsc1 binding. However, instead of observing increased mTORC1 activity, its activity decreases. This reduced activity is likely due to diminished PI3K/Akt signaling when cells grow to confluence.

Defects in TJs are associated with many disease conditions (1). Among these, Crohn's disease and psoriasis show a certain degree of inheritance patterns and connections in close relatives (46). In mice, Tsc1 deficiency caused Crohn's disease-like conditions in intestinal tracts (Fig. 1 D and E) and psoriasis-like symptoms on the skin (Fig. 1J). In human patient samples with TJ-related diseases, we also observed reduced Tsc1 levels in the epithelial junctional membranes (Fig. 7 B and C). These observations suggest that Tsc1 deficiency is associated with TJ-related diseases. In addition, Tsc1 pathogenic point mutations lie within or near the Tsc2-BD (39, 40). These mutations may also affect Tsc1 binding with Myo6, which binds to the same Tsc1 region as Tsc2 does. Thus, while there are no reports of TJ-related pathology in TSC patients, the possibility that some TSC patients may have such symptoms cannot be excluded.

Collectively, this study uncovers a role for Tsc1 in cell adhesion and junctions, thereby expanding our knowledge of Tsc1 beyond its canonical role as an upstream inhibitor of mTORC1. Most importantly, this role of Tsc1 in cell junctions bears an important implication in our understanding of TJ-related disease pathogenesis.

## Materials and Methods

**Materials.** Detailed information for reagents, antibodies, primers, and shRNAs are listed in *SI Appendix, Materials and Resources Table*.

**Human Biopsies.** The study protocols concerning human subjects were consistent with the principles of the Declaration of Helsinki and were approved by the Clinical Research Ethics Committee of Southern Medical University. Patients with Crohn's disease ( $n = 12$ ) and non-Crohn's disease control subjects ( $n = 10$ ) were recruited with written informed consent from the Digestive Division, Nanfang Hospital, Southern Medical University. Patients with psoriasis ( $n = 10$ ) or AD ( $n = 6$ ) and healthy control subjects ( $n = 20$ ) were recruited with written

informed consent from the Department of Pathology, Nanfang Hospital, Southern Medical University. For a detailed description, see *SI Appendix, SI Materials and Methods*.

**Animals.** Animal studies were approved by the Ethical Committee for Animal Research of Southern Medical University and conducted according to guidelines from the Ministry of Science and Technology of China. For a detailed description of animal breeding, tissue preparation, sectioning, fluorescence microscopy, and TEM, see *SI Appendix, SI Materials and Methods*.

**Cellular and Biochemical Assays.** Details of cell culture, plasmids construction, cell transfection, fluorescence microscopy, TEM, Western blotting, IP, sucrose density gradient fractionation, GST pull-down assay, and liquid chromatography-mass spectrometry analyses were described in *SI Appendix, SI Materials and Methods*.

**Quantification and Statistical Analysis.** Quantitation of the colocalization of Tsc1 (or Tsc2) with TJ marker proteins was performed using Image J software (NIH). For cultured cells, >150 cells from three independent experiments (>50 cells per experiment) were quantitated; for tissue specimens, at least 20 sections from six mice (>3 sections for each mouse) were used for quantitation. Statistical analyses were conducted using GraphPad Prism 5.0 software. Data were analyzed using two-tailed  $t$  tests or one-way ANOVA with multiple comparisons, followed by Bonferroni's post hoc test for significance. A  $P$  value of < 0.05 was considered statistically significant. Data were presented as mean values  $\pm$  SEM of at least three independent experiments (for cultured cells,  $n = 3$ ; for mice,  $n = 6$ ). Microscope and Western blot images were representative of at least three independent experiments.

**Data Availability.** All study data are included in the article and/or *SI Appendix*.

**ACKNOWLEDGMENTS.** This work was supported by the National Natural Science Foundation of China (Grants 32071125, 81991511, 81625015, 31771311, and 31600941) and Key Research & Development Program of Bioland Laboratory (Guangzhou Regenerative Medicine and Health Guangdong Laboratory) (Grant 2018GZR110104002).

- N. Sawada, Tight junction-related human diseases. *Pathol. Int.* **63**, 1–12 (2013).
- M. B. Zeisel, P. Dhawan, T. F. Baumert, Tight junction proteins in gastrointestinal and liver disease. *Gut* **68**, 547–561 (2019).
- R. Tokumasu *et al.*, Dose-dependent role of claudin-1 in vivo in orchestrating features of atopic dermatitis. *Proc. Natl. Acad. Sci. U.S.A.* **113**, E4061–E4068 (2016).
- G. H. Liang, C. R. Weber, Molecular aspects of tight junction barrier function. *Curr. Opin. Pharmacol.* **19**, 84–89 (2014).
- L. Shen, C. R. Weber, D. R. Raleigh, D. Yu, J. R. Turner, Tight junction pore and leak pathways: A dynamic duo. *Annu. Rev. Physiol.* **73**, 283–309 (2011).
- E. Steed, M. S. Balda, K. Matter, Dynamics and functions of tight junctions. *Trends Cell Biol.* **20**, 142–149 (2010).
- D. R. Raleigh *et al.*, Tight junction-associated MARVEL proteins marvel3, tricellulin, and occludin have distinct but overlapping functions. *Mol. Biol. Cell* **21**, 1200–1213 (2010).
- K. Shigetomi, Y. Ono, T. Inai, J. Ikenouchi, Adherens junctions influence tight junction formation via changes in membrane lipid composition. *J. Cell Biol.* **217**, 2373–2381 (2018).
- M. Watabe-Uchida *et al.*, alpha-Catenin-vinculin interaction functions to organize the apical junctional complex in epithelial cells. *J. Cell Biol.* **142**, 847–857 (1998).
- J. L. Harder, B. Margolis, SnapShot: Tight and adherens junction signaling. *Cell* **133**, 1118, 1118.e1–2 (2008).
- W. Meng, M. Takeichi, Adherens junction: Molecular architecture and regulation. *Cold Spring Harb. Perspect. Biol.* **1**, a002899 (2009).
- J. L. Maiers, X. Peng, A. S. Fanning, K. A. DeMali, ZO-1 recruitment to  $\alpha$ -catenin—A novel mechanism for coupling the assembly of tight junctions to adherens junctions. *J. Cell Sci.* **126**, 3904–3915 (2013).
- K. A. Orlova, P. B. Crino, The tuberous sclerosis complex. *Ann. N. Y. Acad. Sci.* **1184**, 87–105 (2010).
- D.-F. Lee *et al.*, IKK beta suppression of TSC1 links inflammation and tumor angiogenesis via the mTOR pathway. *Cell* **130**, 440–455 (2007).
- P. B. Crino, K. L. Nathanson, E. P. Henske, The tuberous sclerosis complex. *N. Engl. J. Med.* **355**, 1345–1356 (2006).
- X. Gao, D. Pan, TSC1 and TSC2 tumor suppressors antagonize insulin signaling in cell growth. *Genes Dev.* **15**, 1383–1392 (2001).
- H. Chong-Kopera *et al.*, TSC1 stabilizes TSC2 by inhibiting the interaction between TSC2 and the HERC1 ubiquitin ligase. *J. Biol. Chem.* **281**, 8313–8316 (2006).
- J. Huang, B. D. Manning, The TSC1-TSC2 complex: A molecular switchboard controlling cell growth. *Biochem. J.* **412**, 179–190 (2008).
- A. R. Tee, B. D. Manning, P. P. Roux, L. C. Cantley, J. Blenis, Tuberous sclerosis complex gene products, Tuberin and Hamartin, control mTOR signaling by acting as a GTPase-activating protein complex toward Rheb. *Curr. Biol.* **13**, 1259–1268 (2003).
- C.-H. Lee *et al.*, Constitutive mTOR activation in TSC mutants sensitizes cells to energy starvation and genomic damage via p53. *EMBO J.* **26**, 4812–4823 (2007).
- C. C. Dibble, B. D. Manning, Signal integration by mTORC1 coordinates nutrient input with biosynthetic output. *Nat. Cell Biol.* **15**, 555–564 (2013).
- A. J. Valvezan, B. D. Manning, Molecular logic of mTORC1 signalling as a metabolic rheostat. *Nat. Metab.* **1**, 321–333 (2019).
- D. Mossmann, S. Park, M. N. Hall, mTOR signalling and cellular metabolism are mutual determinants in cancer. *Nat. Rev. Cancer* **18**, 744–757 (2018).
- M. Cornu, V. Albert, M. N. Hall, mTOR in aging, metabolism, and cancer. *Curr. Opin. Genet. Dev.* **23**, 53–62 (2013).
- R. A. Saxton, D. M. Sabatini, mTOR signaling in growth, metabolism, and disease. *Cell* **168**, 960–976 (2017).
- M. Karbowiczek *et al.*, The evolutionarily conserved TSC/Rheb pathway activates Notch in tuberous sclerosis complex and *Drosophila* external sensory organ development. *J. Clin. Invest.* **120**, 93–102 (2010).
- K. Inoki, M. N. Corradetti, K.-L. Guan, Dysregulation of the TSC-mTOR pathway in human disease. *Nat. Genet.* **37**, 19–24 (2005).
- V. Valatas, G. Bamias, G. Kolios, Experimental colitis models: Insights into the pathogenesis of inflammatory bowel disease and translational issues. *Eur. J. Pharmacol.* **759**, 253–264 (2015).
- H. T. T. Nguyen *et al.*, CD98 expression modulates intestinal homeostasis, inflammation, and colitis-associated cancer in mice. *J. Clin. Invest.* **121**, 1733–1747 (2011).
- S. Menon *et al.*, Spatial control of the TSC complex integrates insulin and nutrient regulation of mTORC1 at the lysosome. *Cell* **156**, 771–785 (2014).
- M. J. Gnoth, S. Rudloff, C. Kunz, R. K. Kinne, Investigations of the in vitro transport of human milk oligosaccharides by a Caco-2 monolayer using a novel high performance liquid chromatography-mass spectrometry technique. *J. Biol. Chem.* **276**, 34363–34370 (2001).
- N. Thongon, L.-i. Nakkrasae, J. Thongbunchoo, N. Krishnamra, N. Charoenphandhu, Prolactin stimulates transepithelial calcium transport and modulates paracellular permselectivity in Caco-2 monolayer: Mediation by PKC and ROCK pathways. *Am. J. Physiol. Cell Physiol.* **294**, C1158–C1168 (2008).
- T. L. Plank, R. S. Yeung, E. P. Henske, Hamartin, the product of the tuberous sclerosis 1 (TSC1) gene, interacts with tuberin and appears to be localized to cytoplasmic vesicles. *Cancer Res.* **58**, 4766–4770 (1998).
- J. Ikenouchi, H. Sasaki, S. Tsukita, M. Furuse, S. Tsukita, Loss of occludin affects tricellular localization of tricellulin. *Mol. Biol. Cell* **19**, 4687–4693 (2008).
- C. C. Dibble *et al.*, TBC1D7 is a third subunit of the TSC1-TSC2 complex upstream of mTORC1. *Mol. Cell* **47**, 535–546 (2012).

36. K. C. Liu, R. E. Cheney, Myosins in cell junctions. *Bioarchitecture* **2**, 158–170 (2012).
37. M. P. Maddugoda, M. S. Crampton, A. M. Shewan, A. S. Yap, Myosin VI and vinculin cooperate during the morphogenesis of cadherin cell cell contacts in mammalian epithelial cells. *J. Cell Biol.* **178**, 529–540 (2007).
38. M. Rosner, M. Hanneder, N. Siegel, A. Valli, M. Hengstschläger, The tuberous sclerosis gene products hamartin and tuberin are multifunctional proteins with a wide spectrum of interacting partners. *Mutat. Res.* **658**, 234–246 (2008).
39. A. K. Hodges *et al.*, Pathological mutations in TSC1 and TSC2 disrupt the interaction between hamartin and tuberin. *Hum. Mol. Genet.* **10**, 2899–2905 (2001).
40. Y. Niida *et al.*, Analysis of both TSC1 and TSC2 for germline mutations in 126 unrelated patients with tuberous sclerosis. *Hum. Mutat.* **14**, 412–422 (1999).
41. E. P. Henske, S. Józwiak, J. C. Kingswood, J. R. Sampson, E. A. Thiele, Tuberous sclerosis complex. *Nat. Rev. Dis. Primers* **2**, 16035 (2016).
42. H. L. Sweeney, A. Houdusse, Myosin VI rewrites the rules for myosin motors. *Cell* **141**, 573–582 (2010).
43. A. L. Wells *et al.*, Myosin VI is an actin-based motor that moves backwards. *Nature* **401**, 505–508 (1999).
44. O. C. Rodriguez, R. E. Cheney, A new direction for myosin. *Trends Cell Biol.* **10**, 307–311 (2000).
45. E. R. Geisbrecht, D. J. Montell, Myosin VI is required for E-cadherin-mediated border cell migration. *Nat. Cell Biol.* **4**, 616–620 (2002).
46. M. Cottone, C. Sapienza, F. S. Macaluso, M. Cannizzaro, Psoriasis and inflammatory bowel disease. *Dig. Dis.* **37**, 451–457 (2019).